

Estimate of eddy current effects in the vacuum chamber of the BETA-BEAM RCS

LACHAIZE Antoine

CNRS/IN2P3/IPNO, Orsay, France

16 janvier 2007

The purpose of this paper is to investigate eddy current effects in the vacuum chamber of the Beta-Beam Rapid Cycling Synchrotron. Field components induced by eddy-currents are calculated and their effects on the ring chromaticity and tunes are evaluated. Finally a chromaticity correction scheme preserving a large dynamic aperture is presented.

1 Introduction

Time varying field in magnets of a rapid cycling synchrotron induces eddy currents in vacuum chambers which in turn produce various multipole fields acting on the beam. In dipole magnets, the main generated eddy current field component is a sextupole which modifies the natural chromaticity of the ring. In quadrupoles, the main component is a quadrupolar field which modifies the machine's tunes.

The purpose of this paper is to investigate eddy current effects in the vacuum chamber of the Beta-Beam RCS. Calculations have been made for the updated version of the RCS having a physical radius of 40m. Its major parameters are listed in table 1. Two values of the repetition rate have been envisaged : 10 Hz (baseline scenario) and 20Hz (possible futur upgrade).

| | |
|------------------------------|--------------------|
| Injection energy | 100 MeV/u |
| Extraction energy | 3.5 GeV eq. proton |
| Maximum rigidity | 14.47 T.m |
| Number of FODO cells | 24 |
| Superperiodicity | 3 |
| Repetition rate | 10 Hz or 20Hz |
| Transition gamma | 5.34 |
| Ring circumference | 251.32 m |
| Revolution time at injection | 1.95 μ s |

Table 1 : Main parameters of the ring

2 Induced sextupolar component in the dipoles chambers

For a sinusoidal ramp, the time variation of the magnetic field is given by the equation :

$$B_z(t) = \frac{B_0}{2}(\alpha - \cos(\omega t)) \quad (1)$$

where :

- $B_0 = B_{max} - B_{min}$
- $\alpha = \frac{B_{max} + B_{min}}{B_{max} - B_{min}}$
- $\omega = 2\pi f$
- f is the RCS repetition rate

The general formulae for the sextupolar component in elliptic vacuum chambers is given by : [1], [2] :

$$m = \frac{1}{2B\rho} \frac{\partial^2 B_z}{\partial x^2} = \frac{\mu_0 \sigma e}{h} \frac{\dot{B}}{B\rho} J\left(\frac{b}{a}\right) \quad (2)$$

where :

- $\mu_0 = 4\pi 10^{-7}$ is the vacuum permeability
- $\sigma = 1,3.10^6 \Omega^{-1}.m^{-1}$ is the stainless steel vacuum chamber conductivity
- a is the vacuum chamber half-width
- $h = b$ is the vacuum chamber half-height
- ρ is the dipole bending radius
- e is the chamber thickness

and

$$J\left(\frac{b}{a}\right) = \int_0^{\frac{\pi}{2}} \sin\phi \sqrt{\cos^2\phi + \left(\frac{b}{a}\right)^2 \sin^2\phi} d\phi \quad (3)$$

is a function of the vacuum chamber ellipticity.

Therefore :

$$m = \frac{\mu_0 \sigma e}{h\rho} \frac{\omega \sin(\omega t)}{\alpha - \cos(\omega t)} J\left(\frac{b}{a}\right) \quad (4)$$

Note that in the particular case of two parallel plates with $b \ll a$, ref [3] gives :

$$\frac{\delta^2 B}{\delta x^2} = \mu_0 \frac{\sigma \dot{B} e}{h} \quad (5)$$

So that :

$$m = \frac{1}{2B\rho} \frac{\mu_0 \sigma \dot{B} e}{h} \quad (6)$$

which corresponds to the result given by the equation(2) since, in this case $J\left(\frac{b}{a}\right) = 0.5$. In order to evaluate the consequences of this variable sextupolar component, simulations have been performed with the BETA code [6] which allows the introduction of a sextupolar term β in the data for dipoles.

This β component is defined by :

$$\beta = \frac{\rho^2}{2B} \frac{\partial^2 B}{\partial x^2} = \rho^3 m \quad (7)$$

In order to compensate for this β component, 9 sextupoles per superperiod are installed in the ring (3 in horizontal plane and 6 in vertical plane). The optical functions of the ring for one superperiod with positions of sextupoles are presented in figure 1.

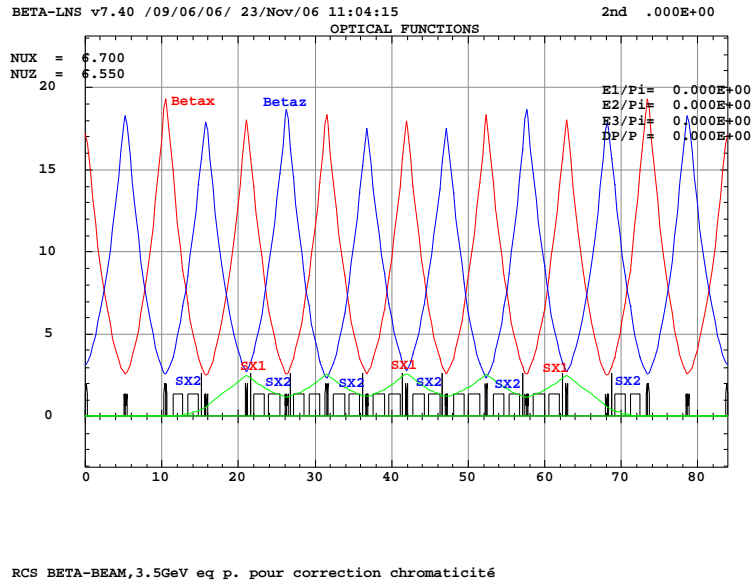


Figure 1 : *Optical functions of the ring and sextupole positions for one superperiod*

2.1 Results for Helium 6 beams

The geometry of the vacuum chamber is defined by the following parameters :

$$a = h = 4cm, b = 5cm, e = 0.3mm.$$

This gives : $J(\frac{b}{a}) = 0.87$

For the Helium ions beam $B_{min} = 0.3321116T$ (at injection) and $B_{max} = 1.082354T$ (at extraction).

Therefore, with a bending radius ρ of 13.369 m we obtain :

$$B(t) = 0.707233 - 0.3751212\cos(2f\pi t) \quad (8)$$

and :

$$m = 0.05 \frac{\sin(\omega t)}{1.885 - \cos(\omega t)} \text{ at } 10Hz \quad (9)$$

$$m = 0.1 \frac{\sin(\omega t)}{1.885 - \cos(\omega t)} \text{ at } 20Hz \quad (10)$$

The sextupolar component variation during the magnetic cycle is given by figures 2a and 2b :

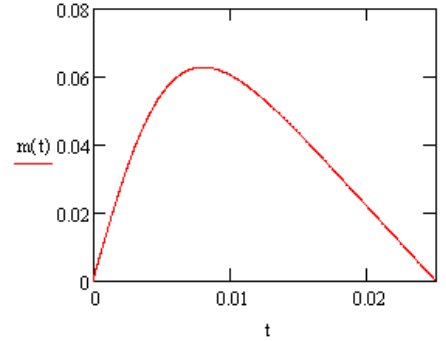
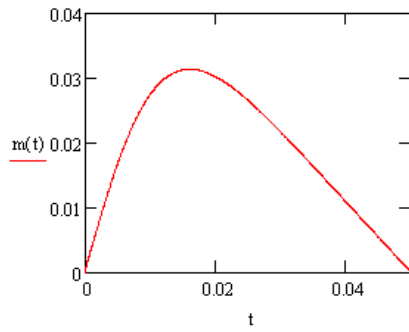


Figure 2a : *Sextupolar component induced by eddy currents during the cycle at 10Hz*

Figure 2b : *Sextupolar component induced by eddy currents during the cycle at 20Hz*

From this result it is possible, using BETA, to calculate the induced chromaticity ξ defined by :

$$\xi = \frac{\frac{\Delta\nu}{\nu}}{\frac{\Delta p}{p}} \quad (11)$$

Figure 3 shows the eddy current induced chromaticity during the magnetic cycle, (natural chromaticity being compensated for by sextupoles and figure 4 shows the total chromaticity (no sextupole correction). In all graphs the black curve corresponds to the horizontal plane and the red curve corresponds to the vertical plane for 10Hz operation, the blue curve corresponds to the horizontal plane and the green curve correspond to the vertical plane for 20Hz operation :

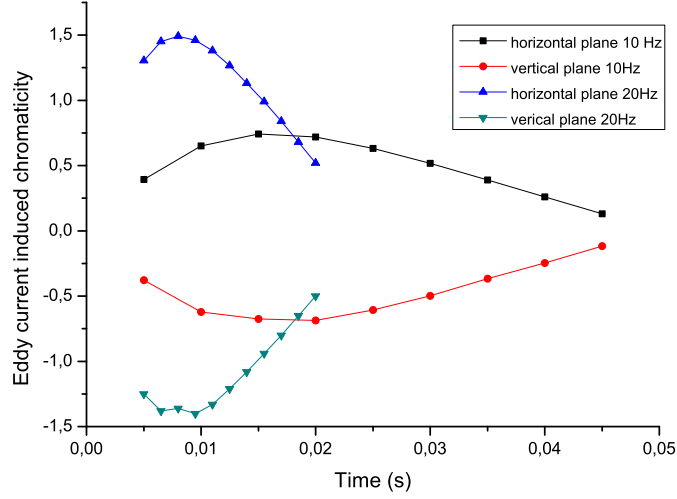


Figure 3 : Eddy current induced chromaticity during the magnetic cycle

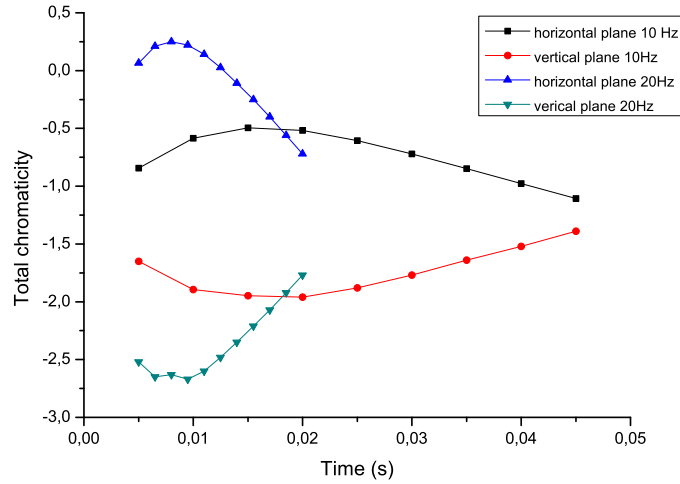


Figure 4 : Total chromaticity during the magnetic cycle

This total chromaticity is then compensated for by sextupoles located in the dispersive sections of the ring (2 families). Their normalized strength Hl with :

$$Hl = \int \frac{1}{2B\rho} \frac{\partial^2 B}{\partial x^2} dl \quad (12)$$

is given in figure 5.

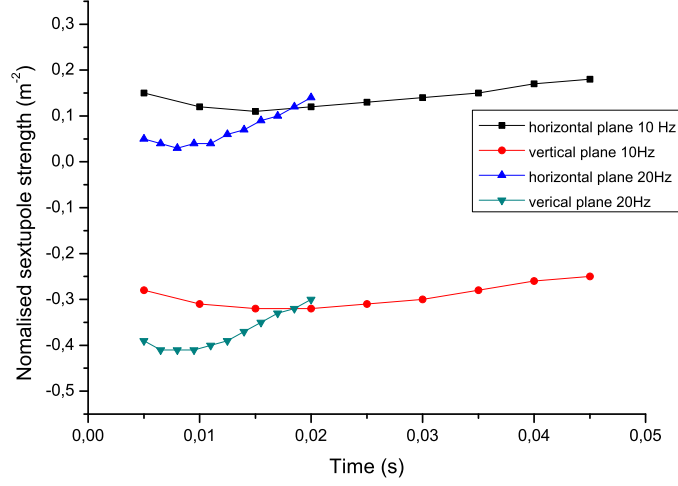


Figure 5 : *Sextupole strength to correct the total chromaticity*

2.2 Results for Neon 18 beams

In the case of Neon ions, the parameter list is exactly the same except for the bending dipole field law which becomes :

$$B(t) = 0.6408104 - 0.441544\cos(2f\pi t) \quad (13)$$

In this way the sextupolar component becomes :

$$m = 0.0536 \frac{\sin(\omega t)}{1.451 - \cos(\omega t)} \text{ at } 10Hz \quad (14)$$

$$m = 0.1072 \frac{\sin(\omega t)}{1.451 - \cos(\omega t)} \text{ at } 20Hz \quad (15)$$

as we can see in figures 6a and 6b :

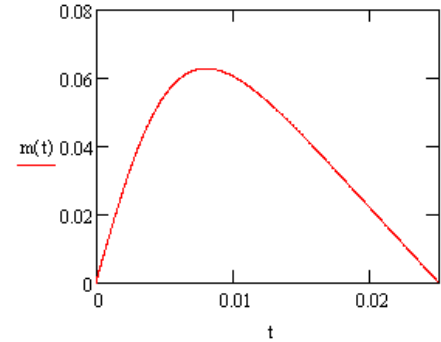
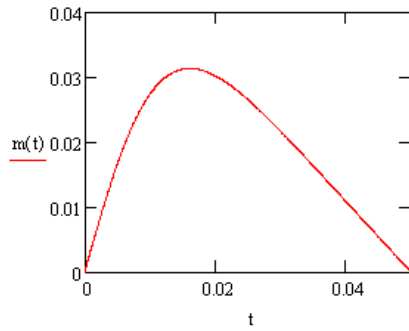


Figure 6a : *Sextupolar component induced by eddy Currents during the cycle at 10Hz* Figure 6b : *Sextupolar component induced by eddy Currents during the cycle at 20Hz*

We then obtain the chromaticity induced by eddy currents :

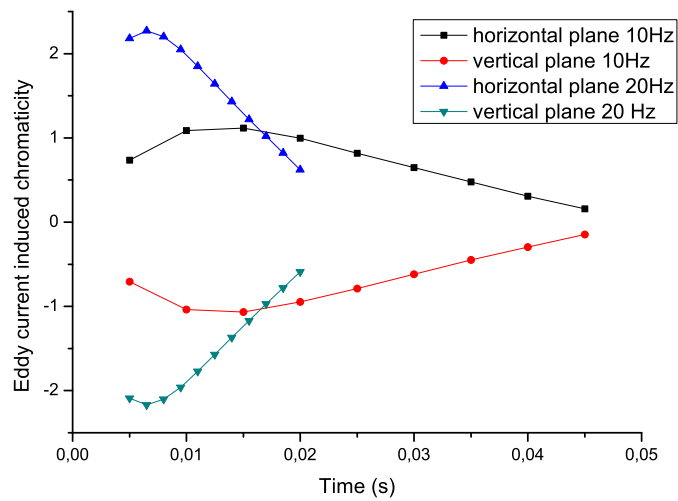


Figure 7 : *Eddy currents induced chromaticity during the magnetic cycle*

And also the total chromaticity during the cycle :

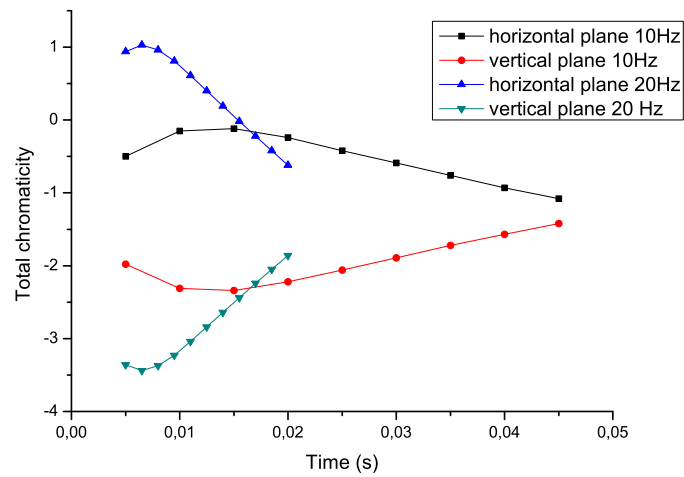


Figure 8 : Total chromaticity during the cycle

Finally, the correction sextupole strength for correcting this total chromaticity during the ramping is given by Figure 9.

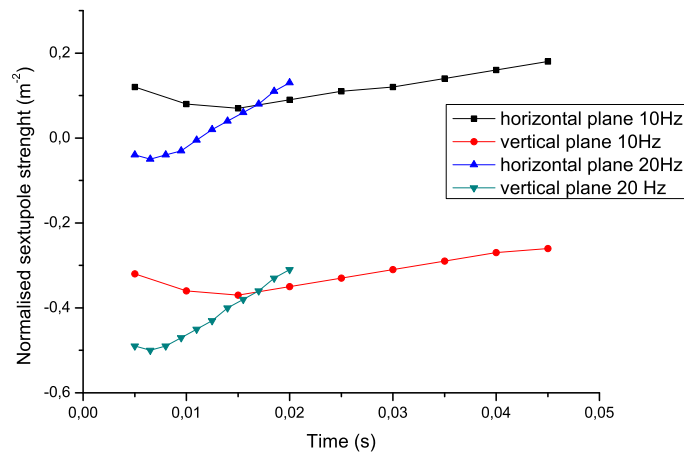


Figure 9 : Sextupoles strength to correct the total chromaticity

3 Induced quadrupolar component in quadrupole vacuum chamber

Eddy current effects in quadrupolar vacuum chambers have been investigated in [4], [5]. For a circular vacuum chamber of \bar{r} medium radius, the relative change of the field gradient is given by :

$$\frac{\Delta G}{G} = -\frac{7}{16}\mu_0\sigma e\bar{r}\frac{\dot{B}_z}{B_z} \quad (16)$$

It is thus possible to evaluate the relative tune shift associated with such a gradient change in a quadrupole using the equation :

$$\frac{\Delta\nu}{\nu} = \beta\frac{\Delta(KL)}{4\pi\nu} \quad (17)$$

with :

$$KL = \frac{GL}{B\rho} \quad (18)$$

where :

- β is the beta function of the ring at the level of the quadrupole
- L is the quadrupole length.

The total tuneshift is given by the sum of each quadrupole contribution of the ring neglecting the optical functions variations .

$$\Delta\nu = \frac{1}{4\pi} \int \beta(s)\Delta K.ds \quad (19)$$

As a exemple we have computed the gradient change induced by eddy currents in an inox circular vacuum chamber of radius $r = 5.5cm$, and having a thickness of $e = 0.3mm$ and a conductivity of $\sigma = 1,3.10^6\Omega^{-1}.m^{-1}$ in the case of He beam.

For these calculation we have used the following parameters :

- $\nu_x=6.7$; $\nu_z=6.55$
- $\beta_x \sim \beta_z \sim 17.5m$ in quadrupole
- Focusing quadrupole strength = $0.749424m^{-2}$
- Defocusing quadrupole strength = $-.719992m^{-2}$

Figure 10 shows the relative gradient change in one focusing quadrupole, the associated horizontal tune shift during the ramping is given by figure 11.

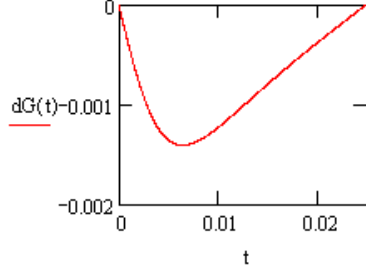


Figure 10 : relative gradient modification during the magnetic field cycle

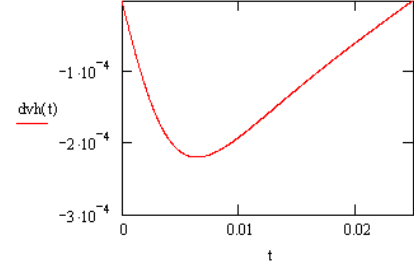


Figure 11 : relative horizontal tuneshift during the magnetic cycle for one quadrupole

In order to obtain the variation over one turn, we add up variations for all focusing or defocusing quadrupoles of the ring. The maximum $\frac{\Delta\nu}{\nu}$ value for one quadrupole is obtained for Neon beam at 20 Hz : $-2.2.10^{-4}$ so :

$\Delta\nu^{max} = 3,5.10^{-2}$ in the horizontal plane for all the ring.

This tune change is very small and does not pose any problem. Moreover this variation is approximatively the same in horizontal and vertical planes because focusing and defocusing quadrupole strength, horizontal and vertical tunes and horizontal and vertical beta functions are not very different.

4 Dynamic aperture

From the point of view of beam dynamics, one of the consequences of the sextupolar component induced in the dipole vacuum chamber is the ring chromaticity modification which induces dynamic aperture modification because of sextupoles compensation. In the vertical plane, the chromaticity is increased and therefore, stronger sextupoles are required for its compensation. As a consequence, a reduction of the dynamic aperture is expected.

The dynamic aperture is presented on figures 12a to 12d. It shows the result of calculations performed with the BETA code for repetition rates of 10Hz and 20Hz. In all cases, the total chromaticity is compensated for by two sextupole families located in the arcs of the RCS.

For both graphs, red curves represent dynamic aperture without eddy currents, green curves correspond to maximal sextupolar component strength and blue curves correspond to a intermediate value at $t=0.03s$ for 10Hz operation and $t=0.014s$ for 20Hz operation.

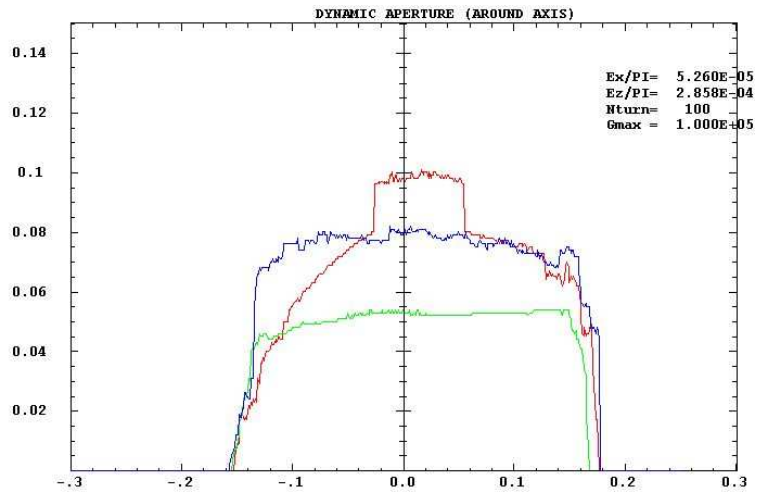


Figure 12a : *Dynamic aperture for Helium ions at 10 Hz*

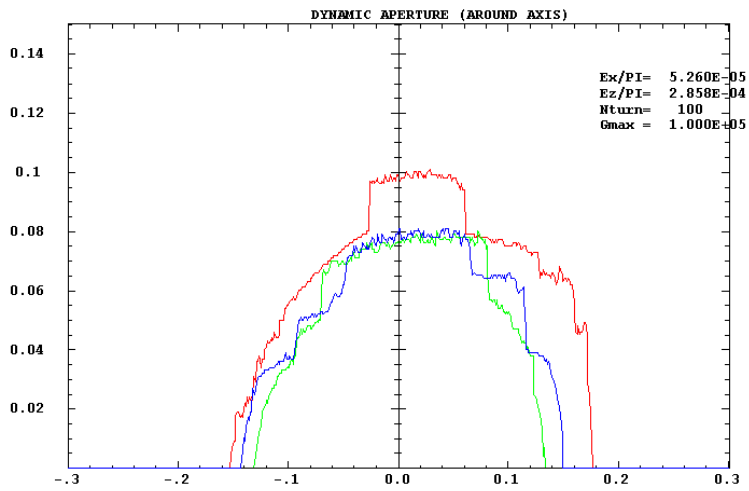


Figure 12b : *Dynamic aperture for Helium ions at 20 Hz*

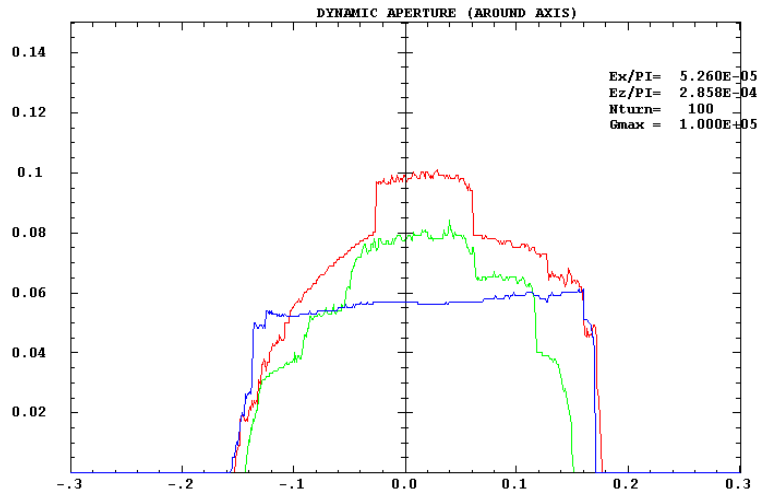


Figure 12c : *Dynamic aperture for Neon ions at 10 Hz*

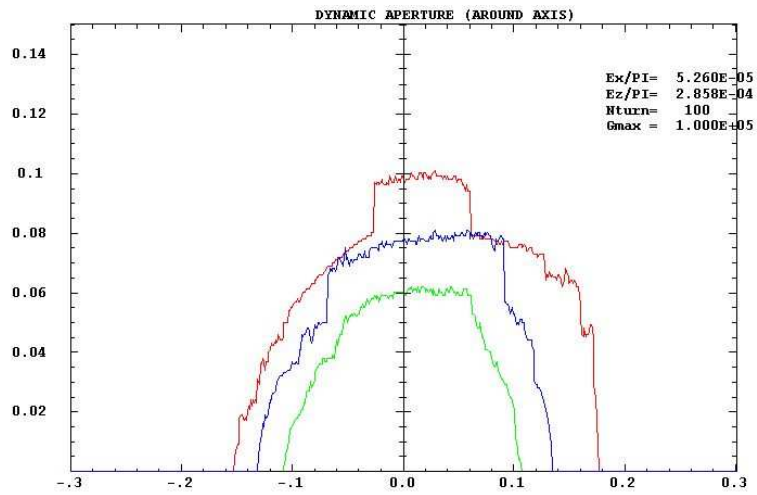


Figure 12d : *Dynamic aperture for Neon ions at 20 Hz*

As one can see, our correction scheme provides, in all cases, dynamic apertures which are larger than the vacuum chamber aperture. Thus, compensation of eddy current effects is not a problem from the point of view of dynamic aperture, even for a repetition rate of 20Hz.

5 Estimate of eddy current power dissipation in the dipole vacuum chamber

As shown in the previous chapter, dynamic aperture is not the figure of merit which gives a limitation for the RCS operation at 20Hz.

This is the reason why calculations have been undertaken to estimate the eddy current power loss in the dipole vacuum chamber and the associated temperature rise. For these calculations, we suppose that the vacuum chamber cross section can be approximate by a rectangle of half-width a and half-height b .

In this case, the power dissipation per unit of length is given by [7], [8] :

$$P_{eddy}/L = 4\dot{B}^2 a^2 e \sigma \left(\frac{a}{3} + b \right) \quad (20)$$

expressed in Watts/meter.

where :

- B is the magnetic field
- a is the chamber half-width = 5cm
- b is the chamber half-height = 4cm
- σ is the chamber's electrical conductivity
- e is the chamber thickness = 0.3mm

The first term corresponds to the power loss in the horizontal walls of the chamber and the second term gives the power loss in the vertical walls. In our case the second term is the most important. Numerically, we obtain the following results for the case of Ne ions acceleration where $\dot{B}_{max} = 55.38$ T/s at 20Hz :

$$P_{eddy}^{max}/L = 199.35W/m(hor.faces) + 478.44W/m(vert.faces) = 677.8 \text{ W/m for Ne at } 20\text{Hz.}$$

$$P_{eddy}^{max}/L = 49.83W/m(hor.faces) + 119.61W/m(vert.faces) = 169.45 \text{ W/m for Ne at } 10\text{Hz.}$$

and the time average power which is dissipated in the chamber during the cycle per unit of length becomes :

$$P_{eddy}/L = 99.67W/m(hor.faces) + 239.2W/m(vert.faces) = 338.9 W/m \text{ for Ne at } 20Hz.$$

$$P_{eddy}/L = 24.915W/m(hor.faces) + 59.8W/m(vert.faces) = 84.7 W/m \text{ for Ne at } 10Hz.$$

This power being significant, calculations have been performed with the code I-DEAS to estimate the vacuum chamber temperature rise [9], [10]. Results are summarized in figure 13. Temperature distributions are given for Ne operation at 10Hz (right) and 20Hz (left).

In both case, a chamber section of 10cm long is represented.

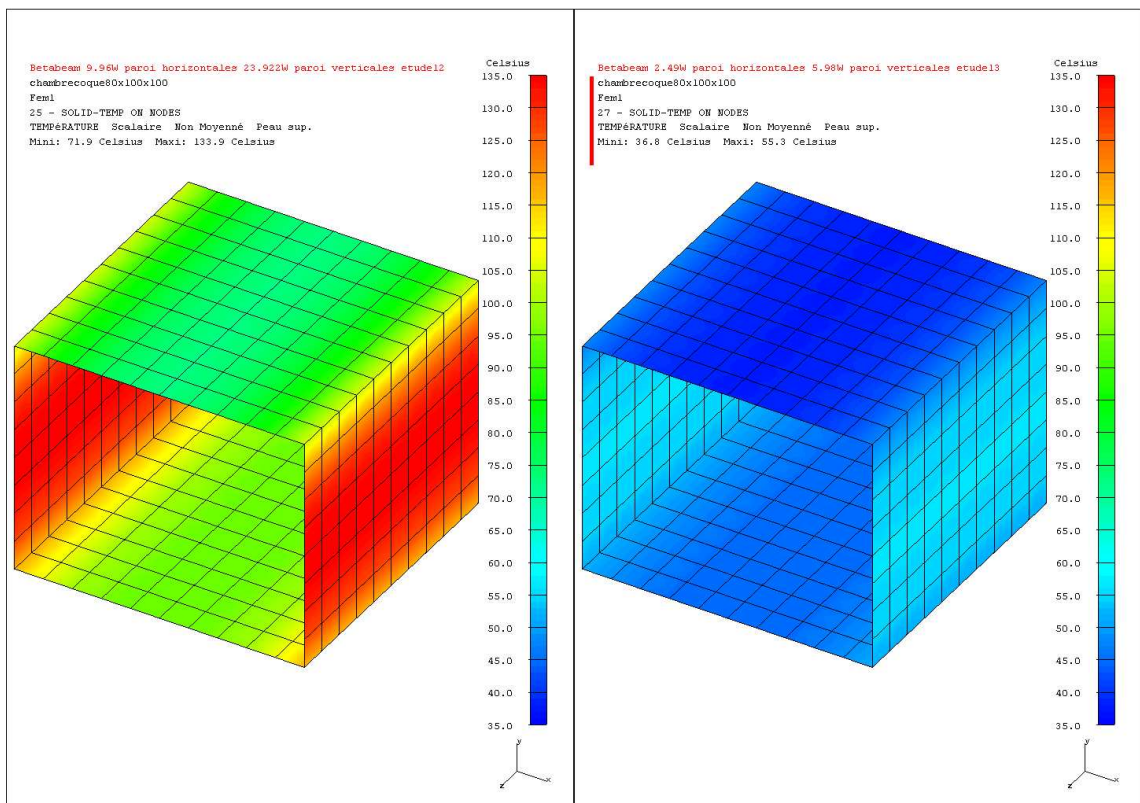


Figure 13 : Chamber heating simulations for 10Hz and 20Hz operation

As we can see, the maximum chamber temperature is below 60°C at 10Hz but is above 130°C at 20Hz. In this last case, detailed technological issues have to be considered to assess the consequences of such a temperature.

6 Acknowledgments

The author wishes to thank A.Tkatchenko for many helpful discussions and advices concerning the bibliography and the analytical calculation of eddy current effects in pulsed magnets vacuum chambers.

We acknowledge the financial support of the European Community under the FP6 « Research Infrastructure Action - Structuring the European Research Area »EURISOL DS Project Contract no. 515768 RIDS.

7 Appendix

Here are presented the values of β component and sextupoles strength during the magnetic cycle for both ions.

| t (s) | β | SX1 (m^{-2}) | SX2 (m^{-2}) |
|-------|---------|------------------|------------------|
| 0.005 | 39.503 | 0.15 | -0.28 |
| 0.01 | 65.265 | 0.12 | -0.31 |
| 0.015 | 74.51 | 0.11 | -0.32 |
| 0.02 | 72.098 | 0.12 | -0.32 |
| 0.025 | 63.38 | 0.13 | -0.31 |
| 0.03 | 51.788 | 0.14 | -0.30 |
| 0.035 | 39.088 | 0.15 | -0.28 |
| 0.04 | 26.067 | 0.17 | -0.267 |
| 0.045 | 13.0186 | 0.18 | -0.25 |

Tableau 1 : β component and correction hexapoles strength HL during the cycle for He ions at 10 Hz.

| t (s) | β | SX1 (m^{-2}) | SX2 (m^{-2}) |
|--------|---------|------------------|------------------|
| 0.005 | 130.66 | 0.0401 | -0.39 |
| 0.0065 | 145.243 | -0.0177 | -0.419 |
| 0.008 | 149.684 | -0.0214 | -0.41 |
| 0.0095 | 146.609 | -0.037 | -0.41 |
| 0.011 | 138.398 | 0.0256 | -0.4 |
| 0.0125 | 126.888 | 0.0509 | -0.39 |
| 0.014 | 113.37 | 0.0799 | -0.37 |
| 0.0155 | 98.702 | 0.105 | -0.35 |
| 0.017 | 83.422 | 0.131 | -0.33 |
| 0.0185 | 67.855 | 0.131 | -0.32 |
| 0.02 | 52.185 | 0.131 | -0.3 |

Tableau 2 : β component and correction hexapoles strength HL during the cycle for He ions at 20 Hz.

| t (s) | β | SX1 (m^{-2}) | SX2 (m^{-2}) |
|-------|---------|------------------|------------------|
| 0.005 | 73.046 | 0.125 | -0.32 |
| 0.01 | 109.386 | 0.08 | -0.36 |
| 0.015 | 111.971 | 0.07 | -0.37 |
| 0.02 | 99.048 | 0.09 | -0.35 |
| 0.025 | 82.338 | 0.11 | -0.33 |
| 0.03 | 64.559 | 0.12 | -0.31 |
| 0.035 | 47.408 | 0.14 | -0.29 |
| 0.04 | 31.072 | 0.16 | -0.277 |
| 0.045 | 15.37 | 0.18 | -0.26 |

Tableau 1 : β component and correction hexapoles strength HL during the cycle for Ne ions at 10 Hz.

| t (s) | β | SX1 (m^{-2}) | SX2 (m^{-2}) |
|--------|---------|------------------|------------------|
| 0.005 | 218.772 | -0.04 | -0.49 |
| 0.0065 | 227.259 | -0.05 | -0.5 |
| 0.008 | 220.447 | -0.04 | -0.491 |
| 0.0095 | 205.162 | -0.03 | -0.47 |
| 0.011 | 185.746 | -0.006 | -0.45 |
| 0.0125 | 164.676 | 0.02 | -0.43 |
| 0.014 | 143.258 | 0.04 | -0.4 |
| 0.0155 | 122.127 | 0.06 | -0.38 |
| 0.017 | 101.543 | 0.08 | -0.36 |
| 0.0185 | 81.564 | 0.11 | -0.33 |
| 0.02 | 62.145 | 0.13 | -0.31 |

Tableau 2 : β component and correction hexapoles strength HL during the cycle for Ne ions at 20 Hz.

Références

- [1] G.Hemmie and J.Rossbach *Eddy Current effects in the DESY II dipole vacuum chamber*, DESY M-84-05 April 84
- [2] F.Lazzourene *Updated lattice for the ELETTRA Booster synchrotron*, ST/M-00/2 April 2001
- [3] M.Sommer *Calcul de la chromaticité introduite par les courants de Foucault à l'injection dans le booster de Soleil*, Note SOLEIL /A/92-24
- [4] J-L.Laclare and G.Leleux *Du problème des courants de Foucault induits dans la chambre à vide des aimants de courbure et des quadrupôles*, note DSS.SOC.RS.73.55
- [5] M.Kobayashi *Note on the Eddy current effects in circular vacuum chambers of dipole and quadrupole magnets*, KEK-72-8 july 1972
- [6] J.Payet *Code BETA*, LNS version ; [ftp ://ftp.cea.fr/incoming/y2k01/beta](ftp://ftp.cea.fr/incoming/y2k01/beta)
- [7] W.Chou, C.Ankenbrandt and E.Malamud *The Proton Driver Design Study*, FERMILAB-TM-2136 December 2000
- [8] Alexander Wu Chao and Maury Tigner *Handbook of Accelerator Physics and Engineering*, 1999 World Scientific Publishing ISBN 9810238584
- [9] F.Launay DA-CNRS/IN2P3/IPNO (private communication). launay@ipno.in2p3.fr
- [10] code I-DEAS, Société EDS Unigraphics Solutions France.